Moun-related bound-state systems from Gaussian expansion method

Presenter:Ting-ting Liu

Collaborators:Yu-xing He, Meng-ke Zheng,Wei-jun Deng
Ling-Yun Dai

School of Physics & Eletronics, Hunan University

May 18,2025

Contents

Research Motivation

- The observation of charged lepton flavor violation (cLFV) in muon decays (*such as* $\mu \rightarrow \gamma e$ *or* $\mu \rightarrow eee$) would constitute an unambiguous signature of physics beyond the Standard Model (BSM)[1]
- Once a dimuonium state is produced it can be studied in detail, allowing for a precision test of QED and a probe of BSM physics. [2]

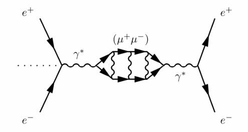

[1] Lorenzo Calibbi. Charged Lepton Flavour Violation: An Experimental and Theoretical Introduction . Riv. Nuovo Cim. 41.2 (2018)

[2]S. J. Brodsky. Production of the Smallest QED Atom: True Muonium(μ^+ mu^-) , Phys. Rev. Lett. 102, 213401 (2009)

Research Motivation

- The magnetic dipole interaction between electrons and (anti)muons bound in muonium gives rise to a hyperfine splitting (HFS) of the ground state which is sensitive to the muon anomalous magnetic moment. [3]

- The proton's charge radius can be precisely determined by measuring the $2S_{1/2}$- $2P_{1/2}$ Lamb shift in muonic hydrogen($\mu^- p^+$) and using its theoretical relationship with the radius[4]

[3] Cédric Delaunay . Towards an Independent Determi nation of Muon g-2 from Muonium Spectroscopy. Phys. Rev. Lett., 127(25):251801, 2021.

[4] Pohl R. Muonic hydrogen and the proton radius puzzle. arXiv:1301.0905

Research Motivation

- Studies of muonic bound-state energy levels promise sustained progress across the intersecting frontiers of particle, atomic, and nuclear physics.

Hyperfine structure

- ★ Test QED
- ★ Fundamental constants
- ★ New physics effects

Potential energy

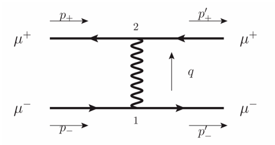

(1)

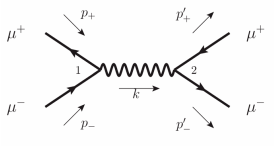

(2)

Ture Muonium Scattering and Annihilation Feynman Diagram

$$\begin{aligned} M_{fi} = & e^2 \left[\bar{u}(p'_-)\gamma^{\mu} u(p_-)\right] D_{\mu\nu}(q) \left[\bar{v}(p_+)\gamma^{\nu} v(p'_+)\right] \\ & - e^2 \left[\bar{u}(p'_-)\gamma^{\mu} v(p'_+)\right] D_{\mu\nu}(k) \left[\bar{v}(p_+)\gamma^{\nu} u(p_-)\right] \end{aligned}$$

$$\begin{cases} u = \sqrt{\frac{E+m}{2E}} \begin{pmatrix} 1 \\ \frac{\mathbf{p}\cdot\boldsymbol{\sigma}}{E+m} \end{pmatrix} |\xi > \\ \bar{u} = \sqrt{\frac{E+m}{2E}} < \xi| \begin{pmatrix} 1 & \frac{-\mathbf{p}\cdot\boldsymbol{\sigma}}{E+m} \end{pmatrix} \end{cases} \qquad \begin{cases} v = \sqrt{\frac{E+m}{2E}} \begin{pmatrix} \frac{\mathbf{p}\cdot\boldsymbol{\sigma}}{E+m} \\ 1 \end{pmatrix} |\eta > \\ \bar{v} = \sqrt{\frac{E+m}{2E}} < \eta| \begin{pmatrix} \frac{\mathbf{p}\cdot\boldsymbol{\sigma}}{E+m} & -1 \end{pmatrix} \end{cases}$$

Born approximation: *amplitude* $\rightarrow$ potential energy

Potential energy

- Potential energy of the scattering diagram

$$U^{(\mathrm{sca})}(\mathbf{p},\mathbf{r}) = -\frac{e^2}{4\pi}\left\{\frac{1}{r} + \frac{\mathbf{p}^2}{2m^2 r} - \frac{3(\boldsymbol{\sigma}_1 + \boldsymbol{\sigma}_2)\cdot(\mathbf{r}\times\mathbf{p})}{4m^2 r^3} + \frac{1}{4m^2 r^3}\left[\boldsymbol{\sigma}_1\cdot\boldsymbol{\sigma}_2 - 3\frac{(\boldsymbol{\sigma}_1\cdot\mathbf{r})(\boldsymbol{\sigma}_2\cdot\mathbf{r})}{r^2}\right] - \frac{2\pi}{3m^2}\boldsymbol{\sigma}_1\cdot\boldsymbol{\sigma}_2\delta(\mathbf{r}) + \frac{\mathbf{r}\cdot(\mathbf{r}\cdot\mathbf{p})\mathbf{p}}{2m^2 r^3} - \frac{\pi}{m^2}\delta(\mathbf{r})\right\}$$

- Potential energy of the annihilation diagram

$$U^{(\mathrm{ann})}(\mathbf{r}) = \frac{e^2}{8m^2}(3 + \boldsymbol{\sigma}_1\cdot\boldsymbol{\sigma}_2)\delta(\mathbf{r})$$

$$\boxed{U^{(}\mathbf{p},\mathbf{r}) = U^{(\mathrm{sca})}(\mathbf{p},\mathbf{r}) + U^{(\mathrm{ann})}(\mathbf{r})}$$

Schrodinger equation

In the two-body problem, we should consider the motion of two particles under their interaction, leading to the Schrodinger equation:

$$(-\frac{1}{2M}\nabla_{\mathbf{R}}^2 - \frac{1}{2\mu}\nabla^2 + V(\mathbf{r}_1 - \mathbf{r}_2))\Psi(\mathbf{R},\mathbf{r}) = E_T\Psi(\mathbf{R},\mathbf{r})$$

Using $\Psi(\mathbf{R},\mathbf{r}) = \psi(\mathbf{r})\phi(\mathbf{R})$ to separate variables, we obtain:

$$\begin{cases} -\frac{1}{2M}\nabla_{\mathbf{R}}^2\phi(\mathbf{R}) = E_c\phi(\mathbf{R}) \\ (-\frac{1}{2\mu}\nabla^2 + V(\mathbf{r}_1 - \mathbf{r}_2))\psi(\mathbf{r}) = E\psi(\mathbf{r}), E = E_T - E_c \\ M = m_1 + m_2, \mu = \frac{m_1 m_2}{m_1 + m_2} \end{cases}$$

$$\boxed{(-\frac{1}{2\mu}\nabla^2 + V(\mathbf{r}_1 - \mathbf{r}_2) - E)\psi(\mathbf{r}) = 0}$$

Gaussian expansion method

Using the multi-Gaussian expansion method, the wave function $\Psi_{lm}(\vec{r})$ is expanded in terms of a series of Gaussian wave functions:

$$\Psi_{lm}(\vec{r}) = \sum_{n=1}^{n_{max}} c_{nl}\phi^{G}_{nlm}(\vec{r})$$

The basis consists of a radial part and an angular part:

$$\phi^{G}_{nlm}(\vec{r}) = \phi^{G}_{nl}(r)Y_{lm}(\hat{r}) = N_{nl}r^{l}e^{-\nu_{n}r^{2}}Y_{lm}(\hat{r})$$

To achieve a high-precision expansion, the optimal set of Gaussian size parameters is a geometric series of parameters:

$$\begin{cases} a = \left(\frac{r_{n_{\max}}}{r_1}\right)^{\frac{1}{n_{\max}-1}} \\ \nu_n = \frac{1}{(r_1 \cdot a^{n-1})^2} \end{cases}$$

Gaussian expansion method

We choose : $\boxed{r_1 = 0.0015 a.u. \quad r_{max} = 1500 a.u. \quad n_{max} = 100}$

The energy eigenvalue equation can be expressed as follows after expanding the eigenstates in terms of Gaussian functions:

$$(-\frac{1}{2\mu}\nabla^2 + V(\mathbf{r}_1 - \mathbf{r}_2) - E)\psi(\mathbf{r}) = 0$$

$$\Downarrow$$

$$\sum_{n'=1}^{N} [(T_{nn'} + V_{nn'}) - EN_{nn'}] c_{n'l} = 0$$

In the equation:

$$N_{nn'} = \langle \phi^G_{nlm} | \phi^G_{n'lm} \rangle = \left(\frac{2\sqrt{\nu_n \cdot \nu_{n'}}}{\nu_n + \nu_{n'}} \right)^{l+\frac{3}{2}}$$

$$T_{nn'} = \langle \phi^G_{nlm} | -\frac{1}{m}\nabla^2 | \phi^G_{n'lm} \rangle = \frac{2(2l+3)\nu_n \cdot \nu_{n'}}{(\nu_n + \nu_{n'})m} \left(\frac{2\sqrt{\nu_n \cdot \nu_{n'}}}{\nu_n + \nu_{n'}} \right)^{l+\frac{3}{2}}$$

Gaussian expansion method

In the equation:

- When $l = 0$

$$
\begin{aligned}
V_{nn'} = & \frac{e^2}{4\pi}\Bigg(\frac{2^{\frac{5}{2}}(\sqrt{\nu_n\nu_{n'}})^{\frac{3}{2}}}{\sqrt{\pi}}\Big\{-\frac{1}{\nu_n+\nu_{n'}}+\frac{1}{m^2}[-\frac{4\nu_{n'}}{\nu_n+\nu_{n'}}+\frac{4\nu_{n'}^2}{(\nu_n+\nu_{n'})^2}]\Big\} \\
& + \frac{5\pi}{2m^2}(\frac{2}{\pi}\sqrt{\nu_n\nu_{n'}})^{\frac{3}{2}} + \frac{7\pi}{6m^2}(\frac{2}{\pi}\sqrt{\nu_n\nu_{n'}})^{\frac{3}{2}}[2S(S+1)-3]\Bigg)
\end{aligned}
$$

- When $l \neq 0$

$$
\begin{aligned}
V_{nn'} = & \frac{2^{2l+\frac{5}{2}}e^2(\sqrt{\nu_n\nu_{n'}})^{l+\frac{3}{2}}l!}{4\pi\sqrt{\pi}(\nu_n+\nu_{n'})^l(2l+1)!!}\Big\{-\frac{1}{\nu_n+\nu_{n'}}+\frac{1}{m^2}[-\frac{\nu_{n'}(2l+3)}{\nu_n+\nu_{n'}}+\frac{2\nu_{n'}^2(l+1)}{(\nu_n+\nu_{n'})^2}] \\
& - \frac{S(S+1)}{2m^2l} + \frac{3[J(J+1)-l(l+1)-S(S+1)][J(J+1)-l(l+1)-S(S+1)+1]}{4m^2l(2l-1)(2l+3)} \\
& - \frac{6S(S+1)(2l^2+2l-1)}{4m^2l(2l-1)(2l+3)} + \frac{l-1}{2m^2} - \frac{\nu_{n'}(2l+1)}{m^2(\nu_n+\nu_{n'})} + \frac{2\nu_{n'}^2(l+1)}{m^2(\nu_n+\nu_{n'})^2} \\
& + \frac{3[J(J+1)-l(l-1)-S(S+1)]}{4m^l}\Big\}
\end{aligned}
$$

True muonium Energy level

- By substituting these matrix elements into the generalized eigenvalue equation and solving with Mathematica, the corresponding energy levels can be obtained.

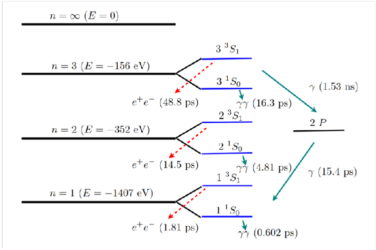

FIG. 1. True muonium levels, lifetimes and transitions diagram for n ≤ 3 (spacing not to scale)[1]

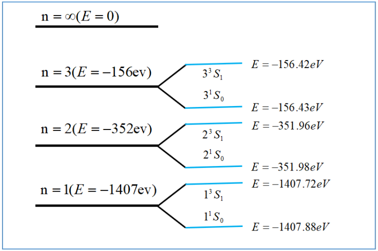

FIG. 2. Energy level diagram of true muonium calculated using the Gaussian expansion method

[1] A. Bogomyagkov EPJ Web Conf. 181 (2018) 01032. arXiv:1708.05819

Muonium Energy level

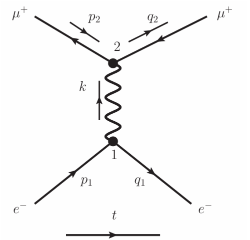

Muonium Scattering Feynman Diagram

$$M = e^2 \bar{u}(q_1)\gamma_\nu u(p_1) D_{\mu\nu}(k) \bar{v}(p_2)\gamma^\nu v(q_2)$$

Born approximation: *amplitude* $\rightarrow$ potential energy

Muonium Energy level

Muonium Potential Energy

$$U(\mathbf{p},\mathbf{k}) = -\frac{e^2}{4\pi}\Bigg\{\frac{1}{r} + \frac{\mathbf{p}^2}{2m_e m_\mu r} - \frac{\pi(m_e^2+m_\mu^2)}{2m_e^2 m_\mu^2}\delta(\mathbf{r}) - \frac{[(2+\frac{m_\mu}{m_e})\boldsymbol{\sigma}_1 + (2+\frac{m_e}{m_\mu})\boldsymbol{\sigma}_2]\cdot(\mathbf{r}\times\mathbf{p})}{4m_e m_\mu r^3}$$
$$+\frac{1}{4m_e m_\mu r^3}[\boldsymbol{\sigma}_1\cdot\boldsymbol{\sigma}_2 - \frac{3(\boldsymbol{\sigma}_1\cdot\mathbf{r})(\boldsymbol{\sigma}_2\cdot\mathbf{r})}{r^2}] - \frac{2\pi\boldsymbol{\sigma}_1\cdot\boldsymbol{\sigma}_2\delta(\mathbf{r})}{3m_e m_\mu} + \frac{(\mathbf{p}\cdot\mathbf{r})(\mathbf{p}\cdot\mathbf{r})}{2r^3 m_e m_\mu}\Bigg\}$$

$$\sum_{n'=1}^{N}[(T_{nn'}+V_{nn'}) - EN_{nn'}]c_{n'l} = 0$$

$$N_{nn'} = \langle\phi^G_{nlm}|\phi^G_{n'lm}\rangle = \left(\frac{2\sqrt{\nu_n\cdot\nu_{n'}}}{\nu_n+\nu_{n'}}\right)^{l+\frac{3}{2}}$$
$$T_{nn'} = \langle\phi^G_{nlm}|-\frac{1}{m}\nabla^2|\phi^G_{n'lm}\rangle = \frac{2(2l+3)\nu_n\cdot\nu_{n'}}{(\nu_n+\nu_{n'})m}\left(\frac{2\sqrt{\nu_n\cdot\nu_{n'}}}{\nu_n+\nu_{n'}}\right)^{l+\frac{3}{2}}$$

Muonium Energy level

Muonium Potential Energy

- When $l = 0$

$$V_{nn'} = -\frac{e^2}{4\pi}\left\{\frac{2^{\frac{5}{2}}(\sqrt{\nu_n\nu_{n'}})^{\frac{3}{2}}}{\sqrt{\pi}}\left[\frac{1}{\nu_n+\nu_{n'}}+\frac{3\nu_n\nu_{n'}-\nu_{n'}^2}{m_e m_\mu(\nu_n+\nu_{\nu_{n'}})^2}-\frac{(m_e^2+m_\mu^2)}{4m_2^2 m_\mu^2}\right.\right.$$
$$\left.\left.-\frac{2S(S+1)-3}{3m_e m_\mu}+\frac{1}{m_e m_\nu}\left[\frac{1}{2}+\frac{\nu_{n'}}{\nu_n+\nu_{\nu_{n'}}}-\frac{2\nu_{n'}^2}{(\nu_n+\nu_{\nu_{n'}})^2}\right]\right]\right\}$$

- When $l \neq 0$

$$V_{nn'} = -\frac{e^2 2^{2l+\frac{5}{2}}(\sqrt{\nu_n\nu_{n'}})^{l+\frac{3}{2}}l!}{4\pi\sqrt{\pi}(2l+1)!!(\nu_n+\nu_{n'})^l}\left\{\frac{1}{\nu_n+\nu_{n'}}+\frac{4\nu_{n'}(l+1)}{(m_e m_\mu)(\nu_n+\nu_{n'})}-\frac{4\nu_{n'}^2(l+1)}{(m_e m_\mu)(\nu_n+\nu_{n'})^2}\right.$$
$$-\frac{l-1}{2m_e m_\mu}+\frac{S(S+1)}{2m_e m_\mu l}-\frac{4+\frac{m_e}{m_\mu}+\frac{m_\mu}{m_e}}{4m_e m_\mu}\frac{[J(J+1)-l(l+1)-S(S+1)]}{2l}-\frac{3}{4m_e m_\mu l}$$
$$*\left(\frac{2S(S+1)(2l^2+2l-1)}{(2l-1)(2l+3)}-\frac{[J(J+1)-l(l+1)-S(S+1)]}{(2l-1)(2l+3)}\right.$$
$$\left.\left.*\frac{[J(J+1)-l(l+1)-S(S+1)+1]}{(2l-1)(2l+3)}\right)\right\}$$

Muonium Energy level

- The same operation was also used to calculate the energy levels of $\mu^+ e^-$.

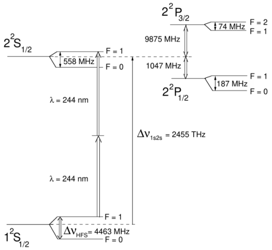

FIG.3. Energy levels of muonium for principal quantum numbers n=1 and n=2[2]

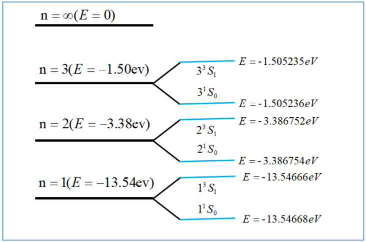

FIG.4. Energy level diagram of muonium calculated using the Gaussian expansion method

[2]Klaus P. Jungmann Muonium. arXiv:physics/9809020v1

Muonic Hydrogen Energy level

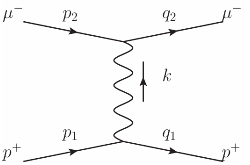

Muonic Hydrogen Scattering Feynman Diagram

$$M = -e^2 \bar{u}(q_1)\gamma_\nu u(p_1) D_{\mu\nu}(k) \bar{u}(q_2)\gamma^\nu u(p_2)$$

Born approximation: *amplitude* $\rightarrow$ potential energy

Muonic Hydrogen Energy level

Muonic Hydrogen Potential Energy

$$
\begin{aligned}
U(\mathbf{p},\mathbf{r}) = & -\frac{e^2}{4\pi}\Bigg\{\frac{1}{r}-\frac{\pi}{2}\left(\frac{1}{m_p^2}+\frac{1}{m_\mu^2}\right)\delta(\mathbf{r})+\frac{1}{2rm_pm_\mu}\left(\mathbf{p}^2+\frac{\mathbf{r}(\mathbf{p}\cdot\mathbf{r})\mathbf{p}}{r^2}\right) \\
& -\frac{1}{4m_p^2r^3}\boldsymbol{\sigma}_1\cdot(\mathbf{r}\times\mathbf{p})-\frac{1}{4m_\mu^2r^3}\boldsymbol{\sigma}_2\cdot(\mathbf{r}\times\mathbf{p}) \\
& -\frac{1}{2m_pm_\mu r^3}\boldsymbol{\sigma}_1\cdot(\mathbf{r}\times\mathbf{p})-\frac{1}{2m_pm_\mu r^3}\boldsymbol{\sigma}_2\cdot(\mathbf{r}\times\mathbf{p}) \\
& +\frac{1}{4m_pm_\mu}\left[\frac{\boldsymbol{\sigma}_1\cdot\boldsymbol{\sigma}_2}{r^3}-\frac{3(\boldsymbol{\sigma}_1\cdot\mathbf{r})(\boldsymbol{\sigma}_2\cdot\mathbf{r})}{r^5}-\frac{8\pi}{3}\boldsymbol{\sigma}_1\cdot\boldsymbol{\sigma}_2\delta(\mathbf{r})\right]\Bigg\}
\end{aligned}
$$

$$
\sum_{n'=1}^{N}[(T_{nn'}+V_{nn'})-EN_{nn'}]c_{n'l}=0
$$

Muonic Hydrogen Energy level

Muonic Hydrogen Potential Energy

- When $l = 0$

$$V_{nn'} = -\frac{e^2}{4\pi}\frac{2^{\frac{5}{2}}(\sqrt{\nu_n\nu_{n'}})^{\frac{3}{2}}}{\sqrt{\pi}}\Big\{\frac{1}{\nu_n+\nu_{n'}} - (\frac{1}{4m_p^2}+\frac{1}{4m_\mu^2}) + \frac{\nu_n^2+\nu_{n'}^2+6\nu_n\nu_{n'}}{m_p m_\mu(\nu_n+\nu_{n'})^2} - \frac{1}{3m_p m_\mu}[2s(s+1)-3]\Big\}$$

- When $l \neq 0$

$$V_{nn'} = -\frac{2^{2l+\frac{5}{2}}e^2(\sqrt{\nu_n\nu_{n'}})^{l+\frac{3}{2}}l!}{4\pi\sqrt{\pi}(\nu_n+\nu_{n'})^l(2l+1)!!}\Big\{\frac{1}{\nu_n+\nu_{n'}} + \frac{4\nu_{n'}(l+1)}{m_p m_\mu(\nu_n+\nu_{n'})} + \frac{1-l}{2m_p m_\mu} - \frac{\nu_{n'}^2(l+1)}{m_p m_\mu(\nu_n+\nu_{n'})^2} - (\frac{1}{8m_p^2}+\frac{1}{8{m_\mu}^2}+\frac{1}{2m_p m_\mu})\frac{J(J+1)-l(l+1)-s(s+1)}{l} + \frac{1}{4m_p m_\mu l}[2s(s+1) - \frac{6s(s+1)(2l^2+2l-1)}{(2l-1)(2l+3)} + \frac{3[J(J+1)-l(l+1)-S(S+1)]}{(2l-1)(2l+3)}] \frac{[J(J+1)-l(l+1)-S(S+1)+1]}{(2l-1)(2l+3)}\Big\}$$

Summary

- We considered two Feynman diagrams of lowest order,and obtained energy levels of Moun-related bound-state systems($\mu^+\mu^-$、μ^+e^-、μ^-p^+). by solving Schrodinger equation using Gaussian expansion method.

- In the future, higher-order corrections will be considered to provide a more precise Moun-related bound-state systems spectroscopy.

Summary

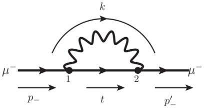

(1) Self-energy

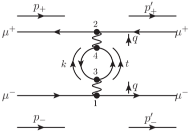

(2) Vacuum polarization

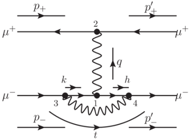

(3) Vertex correction

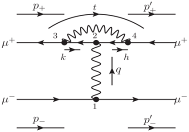

(4) Vertex correction

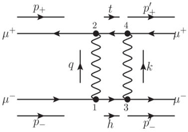

(5) Box diagram

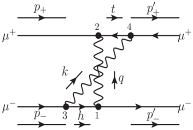

(6) Crossed box diagram

One-loop correction diagram

Thank you for your patience!